A Sensitive Gas Chromatography Detector Based on Atmospheric Pressure Chemical Ionization by a Dielectric Barrier Discharge

Ansgar T. Kirk*, Torben Last and Stefan Zimmermann

Leibniz Universität Hannover, Institute of Electrical Engineering and Measurement Technology, Appelstr. 9A, 30167 Hannover, Germany

*email: kirk@geml.uni-hannover.de *phone: +49 511 762 4864

Abstract

In this work, we present a novel concept for a gas chromatography detector utilizing an atmospheric pressure chemical ionization which is initialized by a dielectric barrier discharge. In general, such a detector can be simple and low-cost, while achieving extremely good limits of detection. However, it is non-selective apart from the use of chemical dopants. Here, a demonstrator manufactured entirely from fused silica capillaries and printed circuit boards is shown. It has a size of 75x60x25 mm³ and utilizes only 2W of power in total. Unlike other known discharge detectors, which require high-purity helium, this detector can theoretically be operated using any gas able to form stable ion species. Here, purified air is used. With this setup, limits of detection in the low parts-per-billion range have been obtained for acetone.

Keywords

Detector; Ionization detector; Atmospheric pressure chemical ionization; Dielectric barrier discharge; Ion mobility

1. Introduction

Gas chromatography is the standard analytical technique for countless applications. Due to this high diversity, there exists an equal variety of different injection techniques, column stationary phases and dimensions as well as detectors. This work will focus on the latter. As gas chromatography itself only provides a temporal separation of the different analytes eluting from the column, the detectors characteristics are crucial for the overall system performance, determining which substances can be detected and in which concentration. A large variety of widely used detectors are based on the ionization of the analyte [1], such as the flame ionization detector (FID) [2,3], the photo ionization detector (PID) [4,5] or the electron capture detector (ECD) [6]. Another variant is the (pulsed discharge) helium ionization detector (HID or PDHID) [7,8], which uses a helium plasma to either ionize the analyte directly, acting as a PID, or through generating free electrons from a dopant, acting as an ECD. All these detectors are quite sensitive, being able to detect substances in the sub-parts-per-million-range (FID), the low parts-per-billion-range (PID) or even down to the low parts-per-trillion-range (ECD). However, an electron capture detector can only measure electron affine substances, limiting this kind of sensitivity to a small group of compounds such as halogens, nitriles or nitro compounds. No counterpart for species which typically form positive ions exists so far.

There is however another ionization method, which offers extremely high sensitivity for both high electron affinity and low ionization energy (or high proton affinity) substances – atmospheric pressure chemical ionization (APCI). Substances which combine high ionization energy with low electron affinity, such as permanent gases, are however not detectable. During this process, first stable so-called reactant ions are formed which then ionize the target molecules through a chemical reaction in the gas phase. It has been successfully employed in both mass spectrometers and ion mobility spectrometers, achieving limits of detection in the low parts-per-trillion-range for most substances that are ionizable this way [9,10]. Highly optimized APCI-MS using long reaction times can

even achieve limits of detection in the low parts-per-quadrillion-range [11,12]. Despite these advantages, there is no simple ionization detector based on atmospheric pressure chemical ionization. This can be attributed to a simple problem – its ionization mechanism is based on charge transfer from one ion forming another ion. Thus, a separation between ions is required as a second step, as the total number of ions remains constant independent from the addition of analytes. This is easy when using a mass or ion mobility spectrometer, but a serious hurdle for a simple detector. Developing such an atmospheric pressure chemical ionization detector (APCID), which is able to provide the sensitivity known from an ECD for both substances which form negative and substances which form positive ions, is the goal of this work.

It should be noted that this working principle is still extremely similar to the one of an ECD, but since electrons and the ions formed from capturing them differ so vastly in mass and size, they can be easily separated in an ECD. Furthermore, the processes ionizing analytes in the ECD and forming the negative reactant ions during APCI are the same. As APCI is meant to work on ions, the use of electron capturing carrier gases is possible unlike in an ECD [13].

2. Operating Principle and Construction

Based on the preceding description, it is clear that for the construction of an APCID, two key components are necessary: A primary ion source which generates reactant ions from the carrier gas and a basic ion separation, which is able to distinguish between these reactant ions and product ions. Furthermore, the ions need to be transported from the ionization source to the separation device with as few losses as possible. An extremely simple setup which is able to provide these requirements is shown in Figure 1.

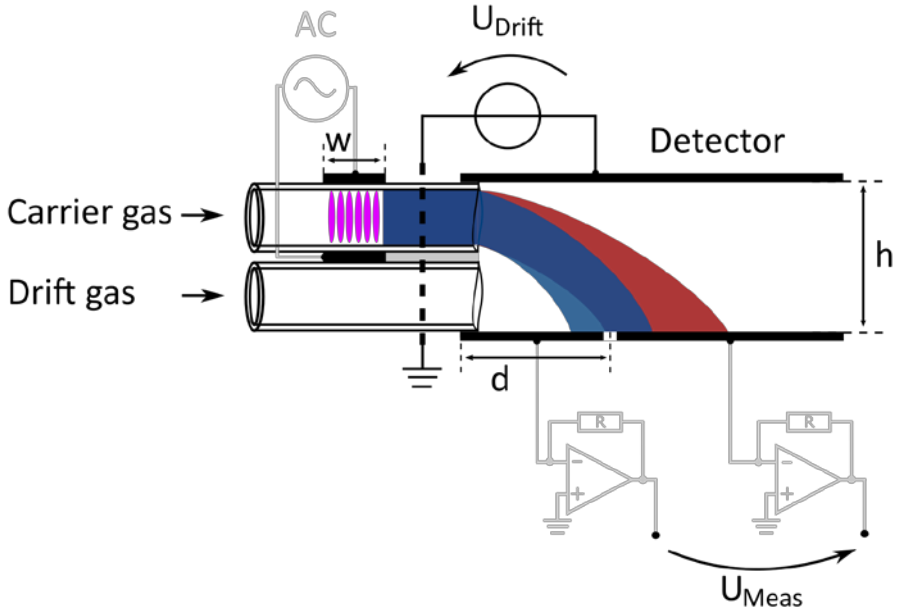

Figure 1: Basic operating principle of the detector. Ions are formed inside the capillary through a DBD, transported by the gas stream and deflected towards the differential detector electrodes by an electric field. Ions of different mobility (blue/red) cause a different current difference between the detector electrodes.

As the primary ion source shown on the left hand side, a dielectric barrier discharge (DBD) is used, as it is simple, cheap and non-radioactive. DBDs are a well-known type of ionization source [14–16], at least when they are operated using helium. To our knowledge, a dielectric barrier discharge using purified air such as the setup in this paper has not yet been used as an ionization device. Generally, an alternating voltage is applied between two electrodes, with at least one of the electrodes being covered by an insulator / dielectric barrier. If the voltage is high enough, a discharge occurs inside the

gap between them, which is self-limited due to charge building up on the dielectric surface. When the AC voltage is reversed, a discharge occurs in the other direction. The two electrodes in our setup are directly applied to a fused silica capillary, which serves as both dielectric barrier and guidance for the gas flow. This is different from many other DBDs and offers several advantages, as neither the gas nor the electron avalanche ever come into contact with the metal of the electrodes, protecting them from wear. A second capillary transports additional clean gas to achieve a constant linear velocity throughout the whole height of the detector setup. The inner diameter of the ionization capillary is 530 µm, while the inner diameter of the lower capillary is 900 µm. Thus, to achieve a constant velocity throughout the height of the detector, the flow in the lower capillary must be about three times as high. The diameter of the ionization capillary was chosen as a compromise since smaller diameters did not deliver a sufficient ion current, but increasing the diameter also increase the size of the initial ion packet. The diameter of the lower capillary is determined by the height of the device. A power supply based on a Royer Converter [18,19] is used to supply a sine voltage of up to 4.5 kV at the resonant frequency determined by the LC-tank formed by the secondary winding of the Royer Converters transformer and the capacitance between the discharge electrodes. Thus, the maximum achievable operating frequency is determined by the electrode geometry, especially by their length *w*. Due to the low volume of the discharge and the resonant drive, the power consumption of the plasma is only 1 W. A grounded electrode is placed in between the DBD and the rest of the setup, both to prevent noise from the discharge to couple to the detector and to protect the ions moving inside the capillary from fringe fields. Depending on the experimental conditions, we observed a reduction of the ion current by more than an order of magnitude if the discharge was badly shielded.

The ion separation device on the right hand side consists of three electrodes, a single deflector electrode on top and a split detector electrode at the bottom. The ions are transported parallel to the electrodes by the gas stream, while an orthogonal electric field deflects them onto the detector electrodes. Such a working principle is similar to the so-called aspiration condenser ion mobility spectrometer [17]. However, instead of sweeping the deflection voltage over a long period of time to obtain an ion mobility spectrum, it is set in a way that the reactant ions hit both plates equally and the current difference between the two plates is measured and plotted over retention time. In the initial state, it is zero. Whenever an analyte elutes from the column, product ions with a different mobility form, which are deflected differently by the voltage and thus strike the detector plates unequally, producing a measurable current difference. This detection scheme is not only advantageous as it should cancel fluctuations in the discharges intensity, but also as small deviations from zero are easier to measure than small deviations from a large number. It can be assumed that due to the minimalistic design, the device will not be able to fully separate the product from the reactant ions, meaning that the sensitivity for an analyte will also depend on the degree of separation between recant and product ions. Here, another advantage of the plasma inside the capillary comes into play, as an extremely thin initial ion packet facilitates separation [17]. The other two important geometrical parameters of an aspiration condenser ion mobility spectrometer and therefore also of the setup employed here are the height of the device *h* and the distance to the detector electrode *d*. According to simulations, they should be chosen to be about equal [20]. Furthermore, increasing them also increases the separation power of the device [20], however at the cost of requiring more drift gas and voltage to maintain the same conditions. In our setup, they are both 1.1 mm based on the dimensions of a successful aspiration condenser ion mobility spectrometer design [17].

Another advantage of such a detector setup is the potentially very short response time. As it is as large as other detectors and not as most spectrometers, it can be placed directly at the end of the column. The internal volume of the short ionization capillary piece, which is about 20mm long, is only

3 µl. Thus, even with a flow of only a few mls/min (milliliter standard per minute), it can be completely exchanged within a few dozen milliseconds. The following ion separation takes place within about 100 µs, leading to a short total time spent inside the device. Dead volumes do practically not exists as the sample is already ionized before it leaves the capillary. Thus, the main limit on response speed is most likely the current amplifier, whose speed should not be chosen faster than necessary to limit the noise. Currently, a rise time of 200 ms is used.

The entire setup of the current demonstrator is, as shown in Figure 2, manufactured from printed circuit boards (PCB) carrying all electronics, power supplies and electrodes. To ensure that no contamination was present on the circuit boards, the output from the system was fed to an ion mobility spectrometer and analyzed. The dimensions of the setup are 75 mm length, 60 mm width and 25 mm height. The only further components needed are a gas supply and a low voltage power supply (12V) to feed the Royer Converter and amplifiers.

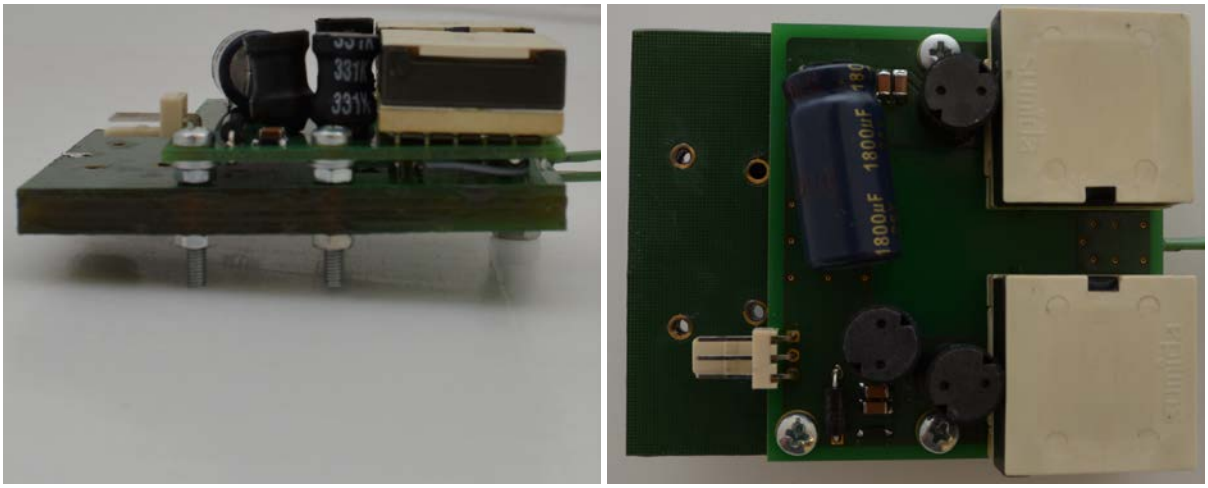

Figure 2: Basic setup of the detector with the HV power supply on top and the transimpedance amplifier at the bottom. It is 75mm long (left to right in the left picture), 60 mm wide (top to bottom in the right picture) and 25 mm high.

Purified air was used as both carrier gas and drift gas, as it is both the standard gas in typical chemical ionization devices such as ion mobility spectrometers and it is ubiquitously available. This is a main difference compared to any other dielectric barrier discharge ionization known to us and an important advantage when considering gas chromatographs for field use or the operating cost in general, as no additional bottled gas such as helium has to be supplied. However, gases which can be exited to metastable states, such as helium or nitrogen, can be expected to deliver higher ion currents due to the possibility of also using penning ionization to generate reactant ions. The typical ionization process occurring during the atmospheric pressure chemical ionization of positive ions are described by the following two equations [10,21].

$$N_2{}^+ + e^- + n\,H_2O + \cdots \rightarrow \cdots \rightarrow N_2 + (H_2O)_n H^+ + \cdots \quad (1)$$

$$(H_2O)_n H^+ + M \rightarrow (H_2O)_{n-1} M H^+ + H_2O \quad (3)$$

In a first step, one of the constituents of the neutral gas is ionized, for example molecular nitrogen in the case of air, which leads to the formation of proton-bound water clusters through several intermediate steps. The number *n* of water molecules bound in this cluster depends on the environmental conditions, such as temperature, pressure and water vapor concentration. In a second step, an analyte molecule can be ionized by this water cluster, typically either through proton transfer or a ligand-switching reaction, where the analyte molecule takes the place of a water molecule in the cluster. This step introduces also a minimum amount of selectivity into the process,

as molecules whose ionization is energetically not favorable will not be ionized. Through the addition of a so-called dopant [22], which forms a new kind of reactant ion which reacts only with a smaller range of substances, some unwanted background signals can be removed.

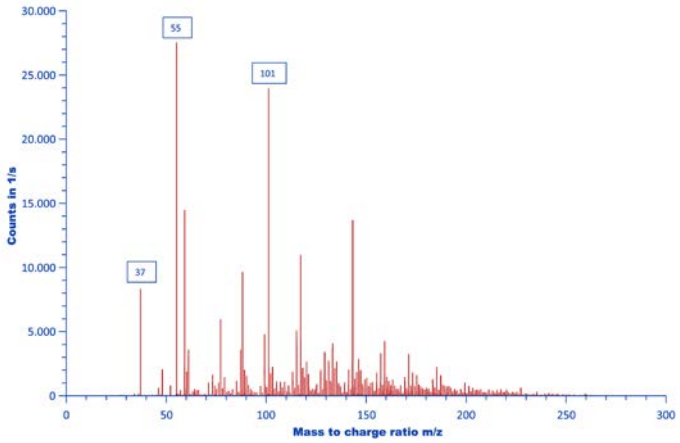

Figure 3: Mass spectrum of the ions generated from the first demonstrator when purified air was used as the discharge gas. Mostly protonated water clusters [$(H_2O)_n(N_2)_mH^+$] are observed.

To ensure that this will be indeed the primary mode of ionization when using our dielectric barrier discharge in air, the ion source of our first demonstrator was coupled to a Bruker micrOTOF II using a custom-build ion interface [23]. The mass spectrum of the generated reactant ions is shown in Figure 3. It should be noted that due to the low mass cutoff of the mass spectrometer, low mass reactant ions are missing and the peak at 37 m/z is most likely already strongly dampened. The three marked peaks are typical water cluster reactant ions [24], being $(H_2O)_2H^+$ at 37 m/z, $(H_2O)_3H^+$ at 55 m/z and $(H_2O)_4N_2H^+$ at 101 m/z. As these ions are in an equilibrium reaction at atmospheric pressure, they all appear together as a single peak inside an ion mobility spectrometer. Thus, despite the large variety of ions present in the background, the most abundant ions by far are water clusters, confirming the suitability of a dielectric barrier discharge operated with purified air to function as a reactant ion source for atmospheric pressure chemical ionization.

In order to avoid confusion, it should be noted some helium ionization detectors are ignited using a dielectric barrier discharge [25,26]. However, they are based on an entirely different ionization principle, as is evident from the fact that they can operate using only a single ion collector electrode. This is only possible when using a type of direct ionization, not with atmospheric pressure chemical ionization, as it requires ion separation. Again, it should be noted that there are helium discharge detectors using multiple collection electrodes [27], but they do not serve to separate different kinds of ions, but to align the chromatograms of identical ions formed at different positions.

3. Initial parametric study of the dielectric barrier discharge

A parametric study of the DBD design was carried out to identify the basic relationships between design parameters and performance. We already presented a first demonstrator at a previous conference [28], where it was shown that the concept works in principle, that increased gas velocities improve the delivered ion current and that simple gas chromatograms can be obtained. This demonstrator was also used here to carry out these studies. In this design, all parts were still hand crafted from metal sheets and thus rather cumbersome. Based on the result of the study, the optimized current demonstrator was developed, which is fully integrated into PCBs as shown by Figure 2. Its main improvements are an integrated transimpedance amplifier to achieve a simpler and more compact setup as well as a more compact design and more compact electrode geometries, which lower the parasitic capacitances and thus increase the achievable discharge frequencies and

voltages. The results from this demonstrator are also shown in the following graphs for comparison. Thus, three different setups were measured: The old demonstrator with 7.5 mm electrodes, the old demonstrator with 15 mm electrodes and the new demonstrator with 7.5 mm electrodes. All measurements were carried out using a flow of 100 mls/min through the discharge capillary and a flow that creates an identical linear velocity through the drift gas capillary. As the original demonstrator is flatter, this flow is 100 mls/min for it, while it is 300 mls/min for the current setup.

The first parametric studies were carried out to quantify the effect of discharge voltage, discharge frequency and electrode length on total ion current and noise current as shown in Figure 4. All these measurands were monitored long enough that the confidence interval for their value is negligibly small. However, this does not include further variations such as long-term instrument drift or assembly variations. The discharge voltage was swept over the voltage range achievable with the load created by the parasitic capacitance of the different designs. Thus, the 7.5 mm electrodes are able to reach higher discharge voltages than the 15 mm electrodes and the new 7.5 mm electrodes reach even further. Furthermore, all three setups were once operated at the maximum frequency that they can achieve, but the old setups were also evaluated at lowered frequencies. This was done to separate possible indirect effects of the electrode length due to the change in maximum discharge frequency caused by their different capacitances. While the total ion current does not directly relate to the achievable limits of detection, it is a good indicator whether a sensitivity improvement is either gained through more primary ions or better efficiency of the ionization or separation. The voltage noise of the amplifier with all voltages including the discharge turned on is less than 10 fA and thus significantly lower than the noise level observed during operation. Thus, the noise current is caused by fluctuations of the ion current reaching the detector.

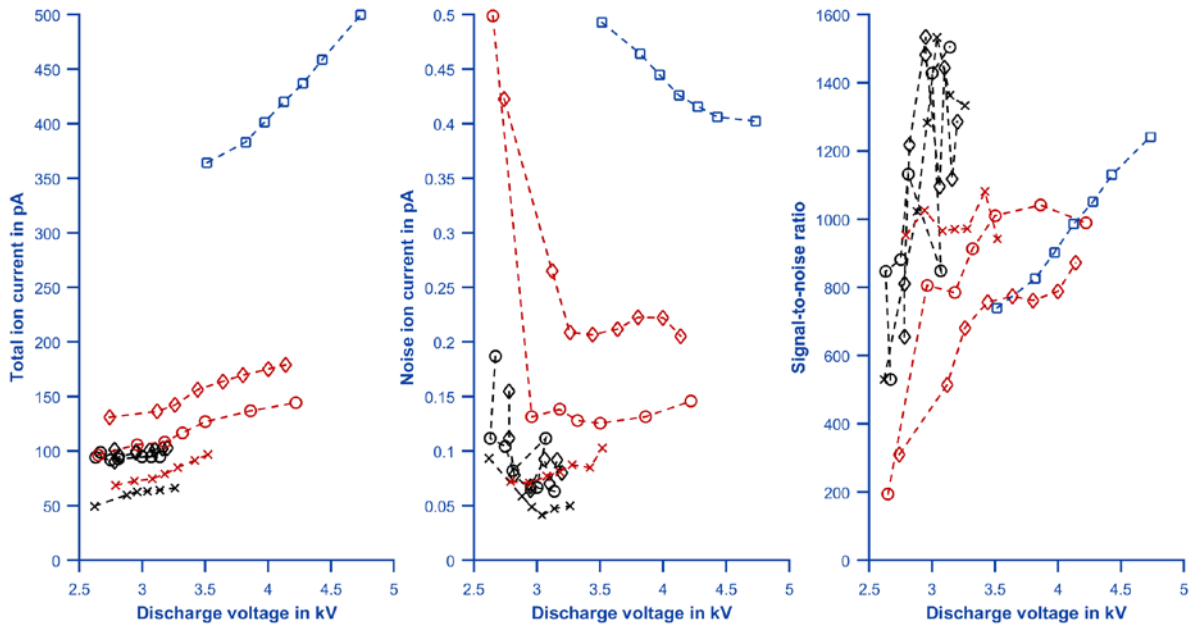

Figure 4: Parametric study of the effects of discharge voltage, discharge frequency and electrode length on total ion current and noise current. Black markers denote the old 15 mm electrodes, red the old 7.5 mm electrodes and blue the new 7.5 mm electrodes. Crosses denote a discharge frequency of 34 kHz, circles 60 kHz, diamonds 67 kHz for the 15 mm and 71 kHz for the 7.5 mm electrodes and squares 82 kHz.

It can be seen that all pairs of electrode lengths and discharge frequencies show the same general behavior when the discharge voltage is swept. The total ion current increases linearly with the discharge voltage, while the noise first shows a sharp drop and then a slight increase for higher voltages. Thus, higher discharge voltages generally produce higher signal-to-noise ratios as shown in

the right panel of Figure 4, giving an advantage to the designs with lower capacitance. Increasing the discharge frequency increases both total ion current and noise current and therefore results in rather similar signal-to-noise ratios, albeit the performance of the higher frequency discharges appears to be slightly inferior for the old demonstrator with an electrode length of 7.5 mm. For the old demonstrator with 15 mm electrodes, the different results overlap strongly, as the lower noise becomes more difficult to measure. Higher electrode length results in lower total ion current, but at the same time even lower noise current, giving the 15 mm electrodes a higher signal-to-noise ratio. Nevertheless, the new demonstrator is able to reach good signal-to-noise ratios despite operating at high frequencies and with short electrodes due to reaching higher discharge voltages.

However, when it comes to the detection of substances, it is not the total ion current that counts, but the sensitivity. For acetone, it has been determined for a selected number of the presented parameter combinations. As shown in the left panel of Figure 5, the discharge voltage has little effect on the sensitivity, despite increasing the ion current delivered. Higher operating frequencies however do increase the sensitivity substantially. Furthermore, the sensitivity is inferior for the 15 mm electrodes when comparing them to the 7.5 mm electrodes at the same frequency. Combined with the already known noise currents, this results in the limits of detection shown in the center panel. Generally, the very low frequency versions fare badly due to their low sensitivity, despite the superior signal-to-noise ratio of their reactant ion current. The medium frequency versions of both the 7.5 and 15 mm electrodes perform the best, reaching limits of detection in the single digit ppb_v-range (parts-per-billion volume). Interestingly, the new demonstrator possesses inferior limits of detection despite offering the best sensitivity of all designs and a high signal-to-noise ratio for the reactant ion current. To evaluate these problems further, the right panel of Figure 5 shows the ratio of sensitivity to total ion current for the different designs, which we named their efficiency. Here, the mid-frequency setups shown the highest values, explaining their superior performance. Both the low frequency setups and the new demonstrator, which operates at higher frequency, show a low efficiency, thus their sensitivity is bad when compared to the total ion current they deliver. As shown before, increased ion current typically occur together with increased noise and thus the efficiency is the key factor to achieve good limits of detection. Finding an explanation why both lower and higher frequencies show a lower efficiency is still part of our current research. While for low frequencies one could expect ion losses to ions reaching the capillary walls during the long periods to be the culprit, this cannot be the case for higher frequencies. However, it was recently shown that the plasma inside a dielectric barrier discharge possess time-dependent properties [29,30], which could be an explanation for a frequency-dependent ionization behavior.

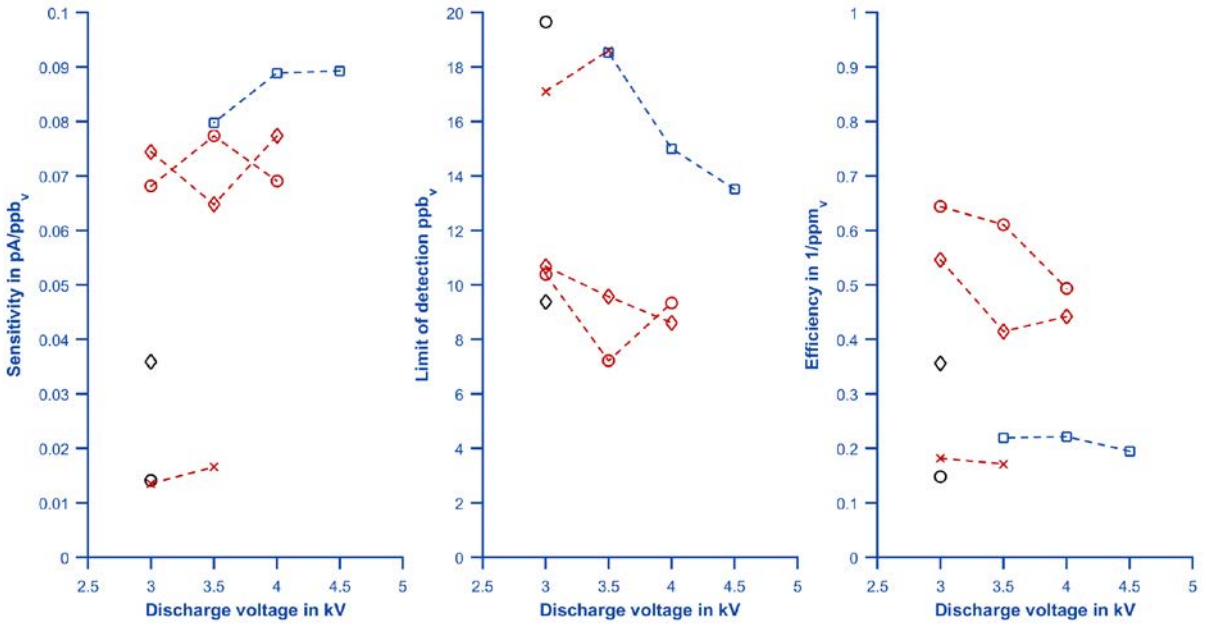

Figure 5: Sensitivity, limit of detection and ionization efficiency (ratio of sensitivity to total ion current) as a function of frequency, discharge voltage and electrode length. The markers are the same as in Figure 4.

4. Experimental results from the current demonstrator

A parameter whose influence is not immediately quantifiable is the gas flow, as it influences not only the discharge, but also the detector properties. First, it carries the ions from the plasma to the detector, thus significantly increasing the ion current for higher flows [28]. However, this also reduces the time the ions formed in the discharge spent together with the analyte molecules, which may result in a diminishing increase in sensitivity. Third, the linear velocity of the gas flow is also a key parameter of the ion separation, as it determines the time spent inside the analyzer and thus the resulting diffusion. Generally, higher linear velocities lead to higher separation power [20]. Thus, flow studies were only carried out using the current demonstrator. First, the total ion current and noise current of the device were characterized with respect to the flow, while the discharge voltage was set to 4.5 kV since this value gave the best performance before. Second, the sensitivity and subsequently the limits of detection and the efficiency were determined for the different flows.

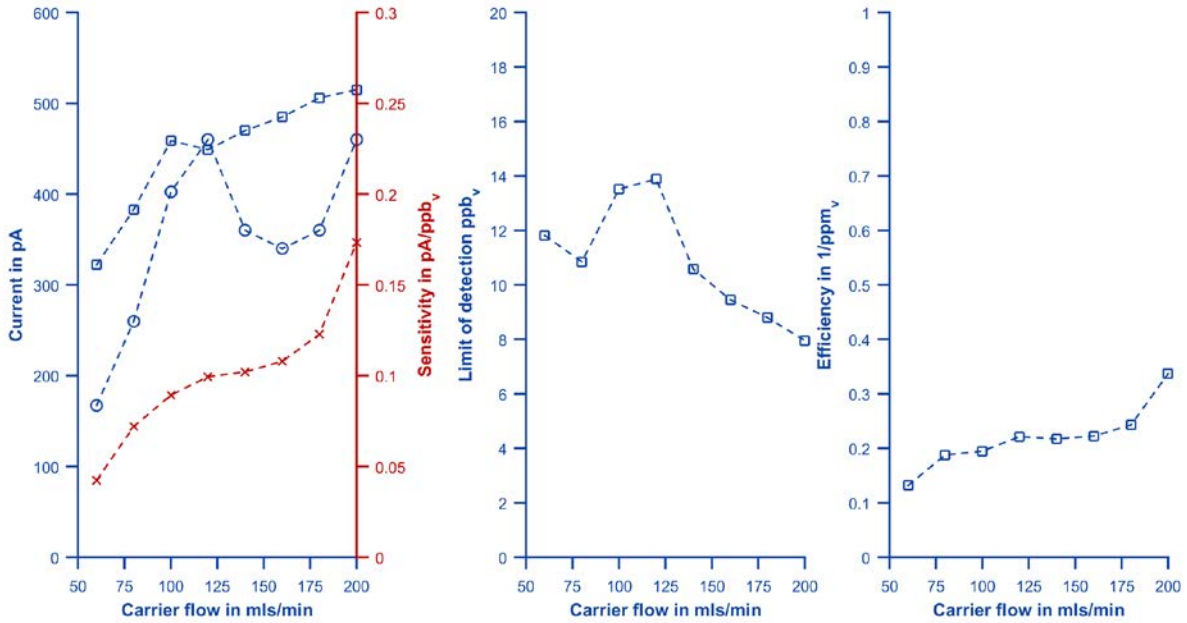

Figure 6: Total ion current, noise current, sensitivity, limits of detection and efficiency of the new demonstrator as a function of the carrier gas flow. In the left panel, the squares denote the total ion current, circles the noise current times thousand and crosses the sensitivity.

The resulting behavior shown in the left panel Figure 6 is rather interesting. The total ion current first grows steeply with the carrier flow, then suddenly shows a small drop between 100 and 140 mls/min and then starts to increase again, but at a much slower rate. Simultaneously, the noise current shows a sharp peak at these flows, with a general growing trend. The same growing trend can be observed for the sensitivity, however it stalls in the flow region between 100 and 140 mls/min. One possible explanation for such a behavior could be a change in flow characteristics, possibly the onset of a turbulence in the system. For even higher flows however, the noise continues to grow at the same speed, but the sensitivity increases rapidly despite only slightly increasing ion currents. This can also be seen in the efficiency shown in the right panel of Figure 6, which start to increase rapidly above 180 mls/min, though flows higher than 200 mls/min could not be set with the current flow controllers. This may be attributed to an improved separation between reactant and acetone ions. These effects combined lead to constantly improving limits of detection with higher flows, except for a spike in the 100 to 140 mls/min region. Thus, the current demonstrator works best when high carrier gas flows are employed. However, there is of course a limit to how much sample gas can be delivered from the gas chromatograph, which would require the use of make-up gas in many applications. This will increase the limits of detection proportionally, giving a better performance to the low flow rates in this case. Another possibility could be coupling this detector to a so-called multi capillary column (MCC), which is easily able to deliver much higher flows of up to several hundred mls/min [31].

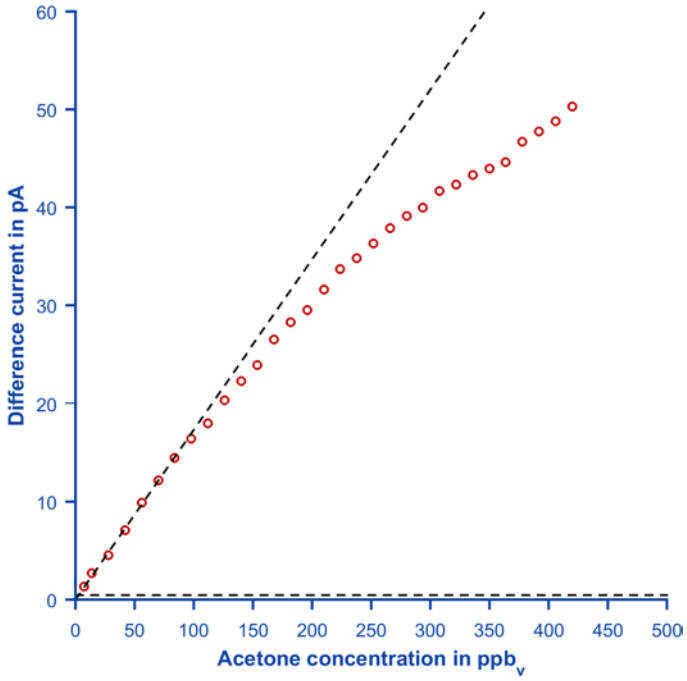

Figure 7: Calibration curve for 200 mls/min flow and 4.5 kV discharge voltage. The black lines show a linear fit and the observed noise level.

Figure 7 shows the observed difference current as a function of the acetone concentration in the sample. It can be seen that for concentrations between 100 and 150 ppb_v, the response begins to deviate from the linear fit. The problem of a limited dynamic range for devices with atmospheric pressure chemical ionization is well known, as ionization can only occur as long as there are reactant ions left. Here however, the difference current is only a fraction of the available current. If the depletion of the reactant ions is the limiting factor for the response, it is most likely that the acetone peak is still not separated well enough from the reactant ion peak, leading to a smaller difference current even though most reactant ions are already depleted. In this case, the increasing sensitivity at high concentrations could be attributed to the formation of a so-called dimer ion [32] containing two acetone molecules. As such an ion is significantly slower, it would be separated better, leading to an increase in sensitivity. In any case, the limited dynamic range is likely to remain a disadvantage of this type of detector. However, as it is non-destructive, it can be coupled with other detector types operating in a different concentration regime.

5. Conclusion

In this paper, a gas chromatography detector based on atmospheric pressure chemical ionization was presented for the first time. Such a detector using a dielectric barrier discharge is generally simple and low-cost, requiring only a few electrodes, purified air and a few watts of electrical power. It could be shown that the operating principle is feasible, achieving limits of detection in the low parts-per-billion range. While this performance is already acceptable, it is still inferior to more sophisticated atmospheric pressure chemical ionization devices, such as ion mobility spectrometers. The two main routes for improvement would be finding a way to increase the available current without increasing the noise and understanding the frequency behavior of the ionization efficiency. If these two limitation can be overcome, future designs should be easily able to measure in the parts-per-trillion range.

6. Acknowledgements

This research did not receive any specific grant from funding agencies in the public, commercial, or not-for-profit sectors.

References

[1] C.F. Poole, Ionization-based detectors for gas chromatography, J. Chrom. A 1421 (2015) 137–153.
[2] I.G. McWilliam, R.A. Dewar, Flame Ionization Detector for Gas Chromatography, Nature 181 (1958) 760.
[3] J. Harley, W. Nel, V. Pretorius, Flame Ionization Detector for Gas Chromatography, Nature 181 (1958) 177–178.
[4] J. Ševčik, S. Krýsl, A photoionization detector, Chromatographia 6 (1973) 375–380.
[5] N. Ostojić, Z. Šternberg, A new photoionization detector for gas chromatography, Chromatographia 7 (1974) 3–5.
[6] J.E. Lovelock, S.R. Lipsky, Electron Affinity Spectroscopy—A New Method for the Identification of Functional Groups in Chemical Compounds Separated by Gas Chromatography 1, J. Am. Chem. Soc. 82 (1960) 431–433.
[7] D.S. Forsyth, Pulsed discharge detector: Theory and applications, J. Chrom. A 1050 (2004) 63–68.
[8] J.E. Lovelock, A sensitive detector for gas chromatography, J. Chrom. A 1 (1958) 35–46.
[9] A.T. Kirk, M. Allers, P. Cochems, J. Langejuergen, S. Zimmermann, A compact high resolution ion mobility spectrometer for fast trace gas analysis, Analyst 138 (2013) 5200–5207.
[10] G.A. Eiceman, Z. Karpas, H.H. Hill, Ion mobility spectrometry. 3rd edn, CRC Press, Boca Raton, 2013.
[11] R.G. Ewing, D.A. Atkinson, B.H. Clowers, Direct real-time detection of RDX vapors under ambient conditions, Anal. Chem. 85 (2013) 389–397.
[12] R.G. Ewing, B.H. Clowers, D.A. Atkinson, Direct real-time detection of vapors from explosive compounds, Anal. Chem. 85 (2013) 10977–10983.
[13] F.W. Karasek, D.M. Kane, Effect of oxygen on response of the electron-capture detector, Anal. Chem. 45 (1973) 576–580.
[14] B. Eliasson, U. Kogelschatz, Modeling and applications of silent discharge plasmas, IEEE Trans. Plasma Sci. 19 (1991) 309–323.
[15] N. Na, M. Zhao, S. Zhang, C. Yang, X. Zhang, Development of a dielectric barrier discharge ion source for ambient mass spectrometry, J. Am. Soc. Mass Spectrom. 18 (2007) 1859–1862.
[16] W. Vautz, A. Michels, J. Franzke, Micro-plasma: a novel ionisation source for ion mobility spectrometry, Anal. Bioanal. Chem. 391 (2008) 2609–2615.
[17] S. Zimmermann, N. Abel, W. Baether, S. Barth, An ion-focusing aspiration condenser as an ion mobility spectrometer, Sens. Actuators, B 125 (2007) 428–434.
[18] A.I. Pressman, K.H. Billings, T. Morey, Switching power supply design, 3rd ed., McGraw-Hill, New York, 2009.
[19] R.L. Bright, G.H. Royer US2783384.
[20] S. Barth, W. Baether, S. Zimmermann, Model-based resolution enhancement of a miniaturized ion mobility spectrometer, IEEE Sensors (2008) 180–183.
[21] R.G. Ewing, G.A. Eiceman, J. Stone, Proton-bound cluster ions in ion mobility spectrometry, Int. J. Mass Spectrom. 193 (1999) 57–68.
[22] E. Waraksa, U. Perycz, J. Namieśnik, M. Sillanpää, T. Dymerski, M. Wójtowicz, J. Puton, Dopants and gas modifiers in ion mobility spectrometry, TrAC, Trends Anal. Chem. 82 (2016) 237–249.
[23] A. Heptner, T. Reinecke, J. Langejuergen, S. Zimmermann, A gated atmospheric pressure drift tube ion mobility spectrometer-time-of-flight mass spectrometer, J. Chrom. A 1356 (2014) 241–248.

[24] G.E. Spangler, J.P. Carrico, Membrane inlet for ion mobility spectrometry (plasma chromatography), Int. J. Mass Spectrom. Ion Phys. 52 (1983) 267–287.
[25] H. Zhu, M. Zhou, J. Lee, R. Nidetz, K. Kurabayashi, X. Fan, Low-Power Miniaturized Helium Dielectric Barrier Discharge Photoionization Detectors for Highly Sensitive Vapor Detection, Anal. Chem. 88 (2016) 8780–8786.
[26] R. Gras, J. Luong, M. Monagle, B. Winniford, Gas Chromatographic Applications with the Dielectric Barrier Discharge Detector, J. Chromatogr. Sci. 44 (2006) 101–107.
[27] H. Cai, S.D. Stearns, Pulsed discharge helium ionization detector with multiple combined bias/collecting electrodes for gas chromatography, J. Chrom. A 1284 (2013) 163–173.
[28] A. Kirk, T. Last, J. Langejuergen, S. Zimmermann, Ein sensitiver Detektor für die Gaschromatographie mittels Ionisation durch eine dielektrische Barrierenentladung, Tagungsband Dresdner Sensor-Symposium 12 (2015) 26–30.
[29] F.D. Klute, A. Michels, A. Schütz, C. Vadla, V. Horvatic, J. Franzke, Capillary Dielectric Barrier Discharge: Transition from Soft Ionization to Dissociative Plasma, Anal. Chem. (2016).
[30] A. Schutz, F.D. Klute, S. Brandt, S. Liedtke, G. Jestel, J. Franzke, Tuning Soft Ionization Strength for Organic Mass Spectrometry, Anal. Chem. 88 (2016) 5538–5541.
[31] V.V. Malakhov, V.N. Sidelnikov, Utkin V.A., Dokl. Akad. Nauk 329 (1993) 749–751.
[32] J. Puton, S.I. Holopainen, M.A. Mäkinen, Sillanpää, Mika E T, Quantitative response of IMS detector for mixtures containing two active components, Anal. Chem. 84 (2012) 9131–9138.